Chapter 5

Cocrystal Technology to Control the Degradation of Histamine H2-receptor Antagonist Drug Famotidine

5.1 Abstract

In this chapter, cocrystallization strategy is used as an effective tool to prevent the degradation of drug famotidine in acidic condition. Famotidine is known for its degradation in the stomach pH environment and therefore we synthesized three cocrystals with xanthine derivatives i.e. theophylline, caffeine and theobromine and analysed the stability issue. The cocrystals are characterized by different spectroscopic, thermal and X-ray diffraction techniques. SCXRD structure of famotidine cocrystal with theophylline has been evaluated. The drug and cocrystal stability are examined under identical conditions. Results suggest enhanced stability of famotidine cocrystal with theophylline and theobromine at pH 1.2. The finding of this work encourages the application of cocrystallization to solve the drug instability issue which is indispensable in a pharmaceutical formulation.

5.2 Introduction

Famotidine (FAM) is a histamine H2–receptor antagonist drug, marketed under the trade name Pepcid [1]. It is used as an effective inhibitor of gastric acid secretion and pepsin for treatment of various kinds of peptic ulcer like gastric and duodenal ulcer, Zollinger-Ellison syndrome, gastro-oesophageal reflux diseases etc. [2,3]. The drug is reported to be 20 times more potent, than other commonly used H2–antagonists like ranitidine and cimetidine, for inhibiting basal and pentagastrin-stimulated gastric acid secretion [4]. However, due to its extremely low solubility and intestinal permeability, it is categorized as a BCS class IV drug [5]. These factors lead to low bioavailability and poor drug efficacy of this drug. Factors like higher polarity and instability are also contributing to its efficacy/ performance [6]. Reports about the decomposition of famotidine are available but a clear picture of the degradation mechanism is yet to understand [6–8]. The drug is unstable both in acidic and basic conditions and formation of three different degradation products of famotidine such as sulfamoyl amide, amide, and carboxylic acid has been reported elsewhere.

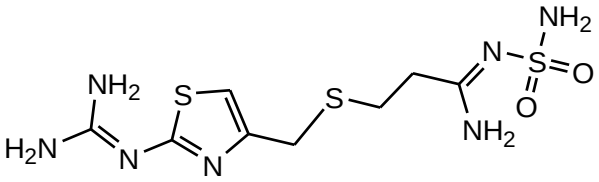

Scheme 5.1 Chemical structure of drug famotidine (FAM)

Under acidic conditions, famotidine degrades rapidly and the concentration of famotidine drops down to 33 % within 1 hour and about 88 % within 3 hours [9]. Two important factors viz. gastric acid and gastric emptying time must be considered to estimate the significance of acid hydrolysis of famotidine in the stomach [10]. It has been established that about 12-57.8% of the drug would be decomposed in case of elder patient within a prolonged period of gastric emptying time (123 min). In case of a younger patient about 5.3-35.7% of the drug would be decomposed within a 50 min of gastric emptying time. Therefore, the stability of this drug is a high demand for better drug efficacy because the degradation of the drug to an inactive metabolite reduces its therapeutic activity [11]. Moreover, the instability of drug molecules may cause toxicity and safety issues. Though the instability was reported nearly 30 years back, approach to preventing the degradation of famotidine is yet to explore.

The effect of carboxymethyl-β-cyclodextrin improving the aqueous solubility, chemical stability and oral bioavailability of famotidine have been reported [9]. In recent times, several researchers demonstrated cocrystal technology as an effective tool to overcome the instability of drug molecules [12–15]. For instance, the cocrystal of succinic acid with temozolomide has been reported to be effective in improving the chemical stability of the drug [16]. This cocrystal exhibits excellent stability for more than six months in high relative humidity. Chemical and physical stability enhancement of vitamin D_3 via cocrystallization also reported [17]. Another recent report shows the cocrystal of nifedipine and isonicotinamide exhibits superior photostability compared to the parent drug nifedipine [18]. CSD analysis reveals that no cocrystal structure of drug famotidine has been reported. Only two conformational polymorphs of famotidine (Form A and B) are reported [19]. One maleate salt of famotidine is reported by Marcos et al. [20]. Enhancement of famotidine dissolution by cocrystallizing with tartaric acid and maleic acid has been demonstrated by Shi et al. in 2013 [21].

Three xanthine derivatives i.e. theophylline, caffeine and theobromine are selected as coformer considering the susceptibility of supramolecular heterosynthons formation. These coformers are also known for their biological activities such as central nervous system stimulator, bronchodilator etc. The isolated cocrystals were characterized by using different analytical techniques such as FT-IR, PXRD, DSC, TGA and SCXRD. The cocrystals were further subjected to a stability study at pH 1.2 mimicking the stomach pH environment and compared with the stability of parent drug famotidine.

5.3 Results and Discussion

5.3.1 Famotidine Decomposition

The degradation of famotidine is highly dependent on experimental pH condition; we opted to optimize the pH condition where famotidine will show major degradation under physiological condition. A UV-visible study has been carried out by considering different media like aqueous, acidic and basic comprising different pH. The concentration of famotidine was monitored for a time span of 20 days. It has been observed that famotidine remained mostly unaffected and approximately 80-90% of its original concentration persist both in aqueous and basic condition up to 20 days. However, famotidine is more susceptible to acidic hydrolysis, which further leads to its degradation. Therefore, to inspect the optimal acidic pH value at acidic condition, λ_{max} shifting of famotidine was monitored within the pH range of ~1.2-6.2 **(**Appendix Figure A.8**).** The change in λ_{max} value is found to be more significant at higher acidic condition i.e. pH~1.2, which signifies a greater extent of degradation of famotidine at this condition. Therefore, the overall study concentrates mainly on this condition and stability experiments are primarily carried out considering the pH of 1.2.

5.3.2 Characterization of Degradation Product

The degraded product of famotidine at pH 1.2 is extracted for comparison and thoroughly characterized (details are given in experimental section) and compared with FAM. For clarity, we assign the degraded product as FAM_D. The FT-IR spectra of famotidine and its decomposed material under acidic condition are shown in Figure 5.1. The entirely different FT-IR spectra of FAM and FAM_D indicate the phase transformation of famotidine at pH 1.2. The appearance of a new peak near 1686 cm^{-1}

indicates the generation of C=O group for the decomposed material. The absorption peak that appears at 3383 cm^{-1} is attributed to the N–H stretching vibration of the primary amide of the decomposed material. ^{1}H and ^{13}C NMR studies also confirm the degradation of famotidine at pH 1.2. Particularly, the appearance of new ^{13}C-NMR signals at 178 ppm adequately distinguishes the formation of FAM_D under pH 1.2. However, we were unable to isolate suitable quality crystals for SCXRD data collection of FAM_D.

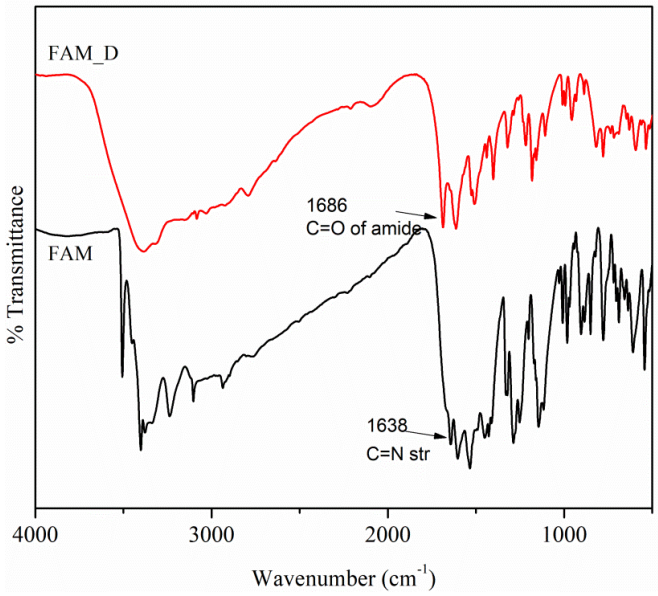

Figure 5.1 FT-IR spectra of pure famotidine and its decomposed product under pH~1.2.

To confirm the instability of famotidine under acidic conditions, we performed a slurry experiment at pH~1.2 HCl conditions. The solid material retrieved from the slurry is analysed by PXRD. The comparison of experimental PXRD patterns of FAM, FAM_D and the slurry materials are shown in Figure 5.2. PXRD pattern of FAM_D exhibits difference in some of the major peak positions and pattern of intensities from that of pure famotidine. Particularly the appearance of new peaks near the 2θ range of 9.34, 12.31, 16.30, 26.45, 34.01, 41.92 and 45.5 signifies a new phase probably the degradation product of famotidine. The PXRD pattern obtained from the slurry experiment is exactly similar to that of FAM_D.

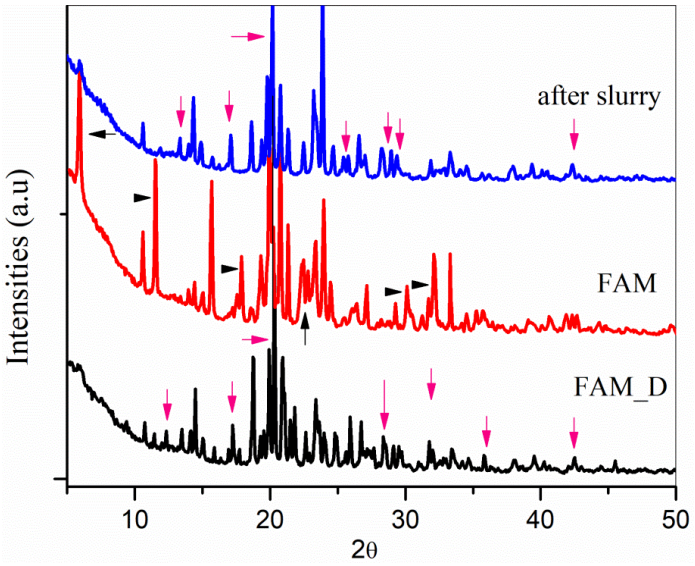

Figure 5.2 Comparison of PXRD patterns for pure famotidine, FAM_D and the material obtained from the slurry experiment at pH 1.2.

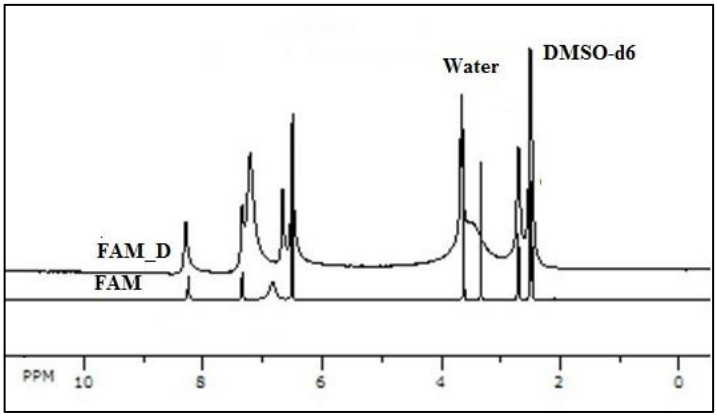

Figure 5.3 ^{1}H-NMR spectra comparisons of famotidine (FAM) and its degradation product (FAM_D).

5.3.3 Kinetics of Famotidine Degradation

The degradation rate famotidine in aqueous medium follows the pseudo-first order kinetics over the pH range of 1-11 [22]. The rate of decomposition of famotidine, under the present condition, studied spectrophotometrically at ambient condition by monitoring the absorption (A_{obs}) of famotidine at 286 nm as a function of reaction time (t) by following equation i.e. ln $[A_t]/[A_0]$ =-kt ; Where $[A_0]$ and $[A_t]$ are the absorbance at time "t" and at zero time respectively. The rate constant (k) for famotidine is found to be 4.93 $X10^{-3}$ min^{-1} (Figure 5.4**)**. The change absorption spectra of famotidine at 1.2 pH conditions with time have been monitored and given in Appendix Figure A.9.

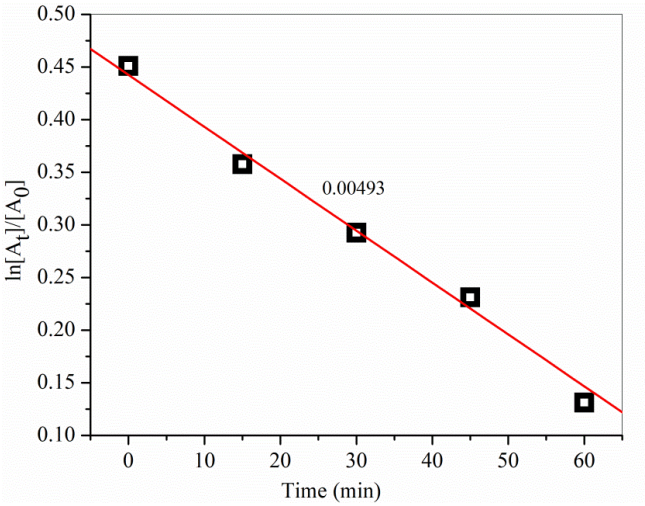

Figure 5.4 Plot of $\ln[A_t]/[A_0]$ vs. time required during hydrolysis under pH~1.2 conditions.

After analyzing the degraded material extracted after 1 hour of slurry at pH 1.2, we propose a mechanistic pathway for the hydrolysis of famotidine that involves the following basic steps as shown in Scheme 5.2. Acid hydrolysis of amidine moiety followed by protonation leads to the reduction of amidine –C=N. Further transfer of proton takes place from the hydronium ion to amine to generate ammonium ion, which is a good leaving group. In the next step, the lone pair on oxygen converts the sp^3 carbon centre to sp^2 by eliminating ammonia generating the degraded product FAM_D. To inhibit the acidic degradation of famotidine crystal engineering principles are applied to formulate FAM as pharmaceutically relevant multicomponent systems such as cocrystal and demonstrated below.

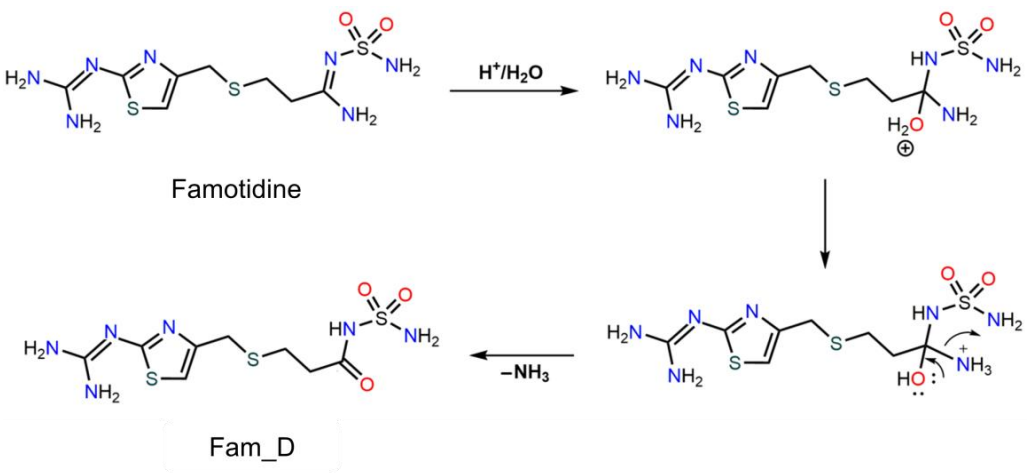

Scheme 5.2 Plausible mechanism of famotidine hydrolysis at pH 1.2

5.3.4 Synthesis of Cocrystal

After deliberate examination of famotidine decomposition at different experimental conditions and identifying its relative decomposition site, cocrystallization technique is explored to prevent the degradation of it. The presence of four hydrogen bond donors and eight hydrogen bond acceptors count makes famotidine an ideal candidate for cocrystallization. The xanthine coformers also exhibit complementary hydrogen bonding sites. Thus, the formation of cocrystals is predictable based on the probability of different heterosynthon formation. Accordingly, liquid-assisted mechanochemical grinding is used to synthesize three cocrystals of famotidine as shown in Table 5.1. The details of the synthesis procedure are given in experimental sections.

Table 5.1 Synthesized cocrystal of drug famotidine with three xanthine derivatives

Drug	Coformer	Cocrystal
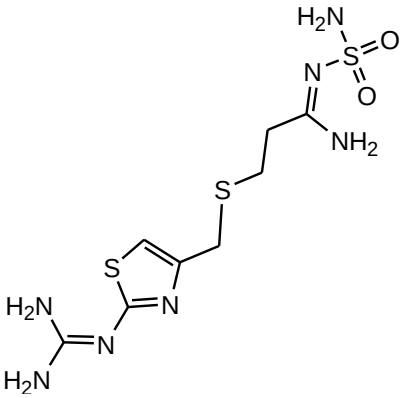 Famotidine (FAM)	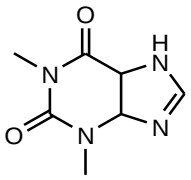 Theophylline (THP)	FAM.THP
	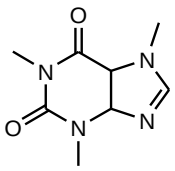 Caffeine (CAF)	FAM.CAF
	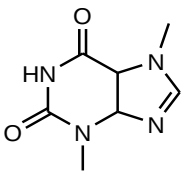 Theobromine (THB)	FAM.THB

5.3.5 Cocrystal Characterization

The synthesized cocrystals are characterized by using FT-IR, PXRD, DSC and SCXRD techniques (details are in experimental section). FT-IR spectra for the cocrystals are shown in Figure 5.5.

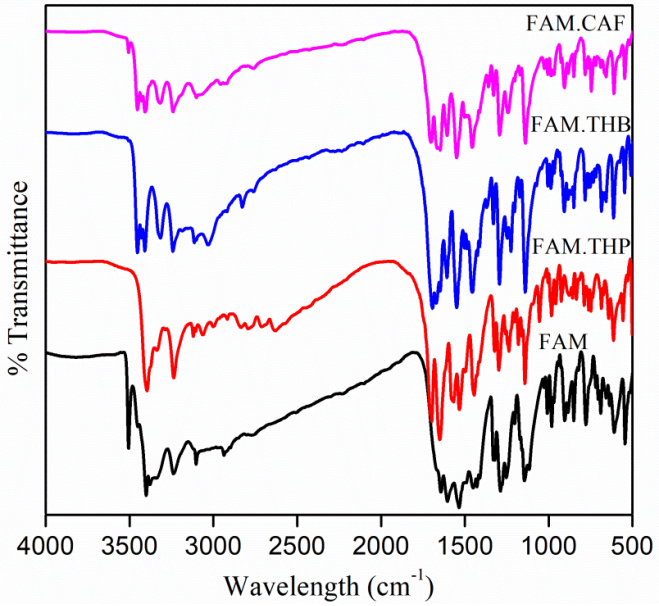

Figure 5.5 FT-IR spectra comparison of famotidine (FAM) and its cocrystals.

Significant lowering of the N–H_{str} frequency indicates the formation of cocrystals. The –C=O group absorption is expected for the xanthine coformers at around 1710 cm^{-1}. However, they appear at lower frequency region in the cocrystals due to the formation of extended intermolecular hydrogen bonding. SO_2 stretching frequencies are observed at 1139, 1131 and 1139 cm^{-1} for of the cocrystals FAM.THP, FAM.CAF and FAM.THB respectively. A substantial lowering of SO_2 stretching frequencies further suggests the cocrystal formation.

Thermal analysis and PXRD experiments are further performed to confirm the cocrystallization. The melting onset temperatures of all three cocrystals are found to be different from that of pure famotidine and their respective coformers (Figure 5.6). Sharp distinct endotherms for each cocrystal manifest the phase purity of the materials. Recrystallization of FAM.THP followed by the melting endotherm may be due to phase transformation into an unknown form and it is beyond the scope of this study. Moreover

minor endothermic disturbances for FAM.THP cocrystal has been observed at around 80 °C, probably because of surface solvent. To confirm the phase stability of the cocrystal a variable temperature PXRD (VT-PXRD) analysis has been performed up to 100 °C and presented in the subsequent section. The features of FAM.CAF cocrystal after melting endotherm represent thermal decomposition. A melting point comparison of cocrystals with their starting materials is depicted in Table 5.2.

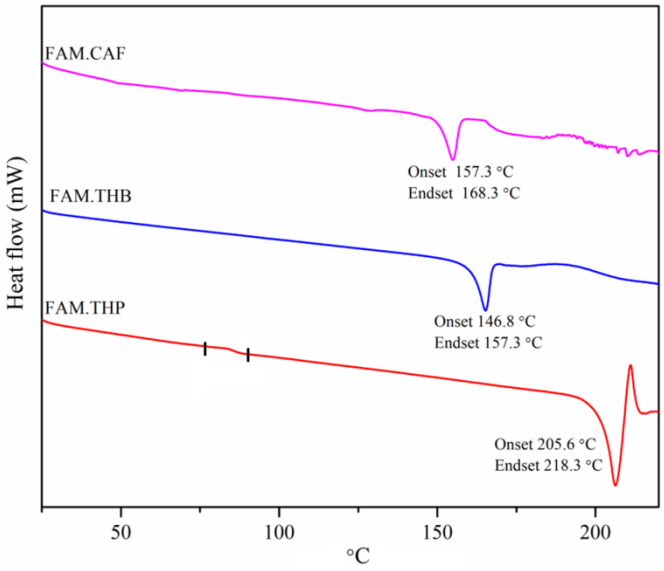

Figure 5.6 DSC endotherms representing the melting onset temperature of famotidine cocrystals.

Table 5.2 Melting point comparison of the cocrystals with their parent compounds.

Drug	Coformer	Coformer MP (°C)	Cocrystals	Cocrystal MP (°C)	
				Onset	Peak
FAM [MP~ 163-165 °C)]	THP	272-273	FAM.THP	205.6	218.3
	CAF	235-237	FAM.CAF	157.3	168.3
	THB	345-350	FAM.THB	146.8	157.3

The PXRD patterns of all three cocrystals show entirely different phases from that of pure famotidine and their respective coformer (Figure 5.7). The stacked plots comparing the cocrystals PXRD patterns and their respective starting materials PXRD patterns are shown below. The experimental PXRD pattern of FAM.THP is compared with the simulated pattern that generated from single crystal X-ray structure and found in good agreement.

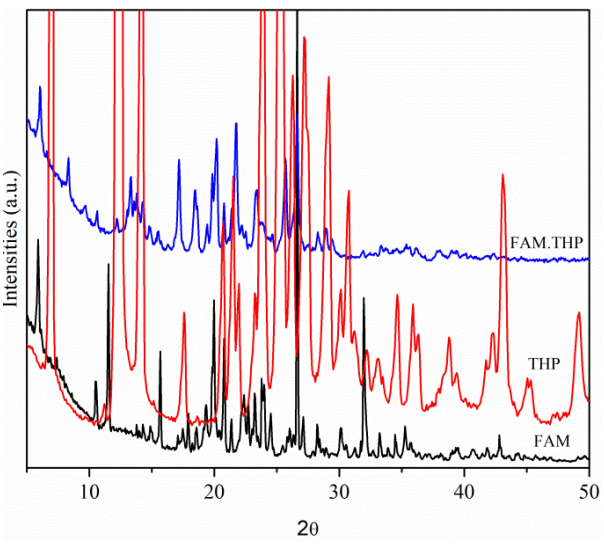

(a)

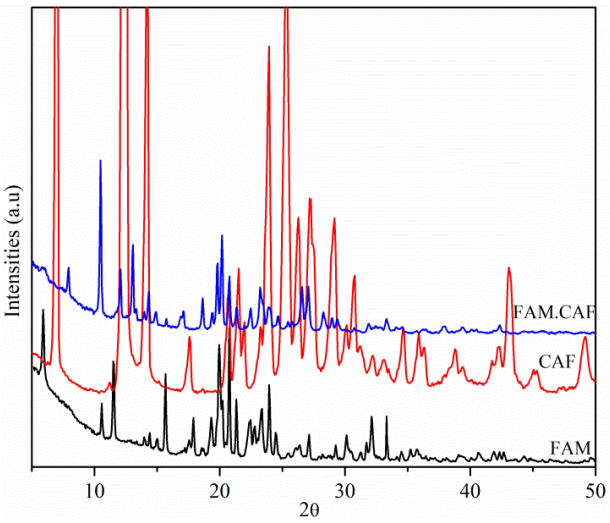

(b)

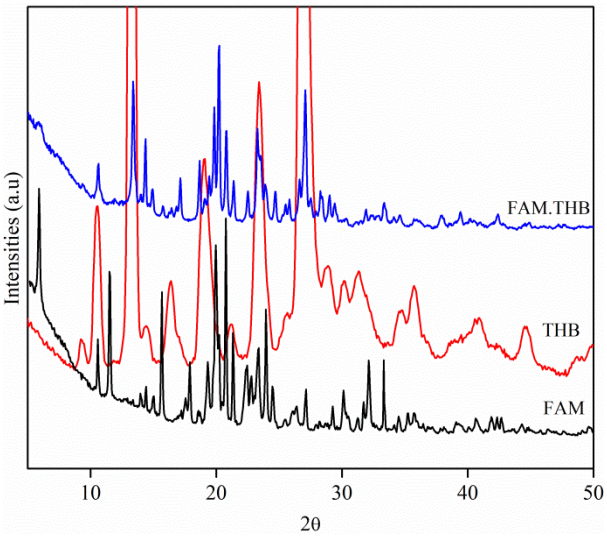

(c)

Figure 5.7 PXRD patterns of famotidine cocrystals of demonstrates new cocrystal phase entirely different from starting material PXRD patterns.

VT-PXRD analysis of FAM.THP established the thermal stability of FAM.THP cocrystal in the solid state up to 100 ºC (Figure 5.8). VT-PXRD patterns and intensities of FAM.THP cocrystal does not show any kind of spectral change up to 100 ºC confirming the phase stability. For comparison, VT-PXRD of FAM is also performed.

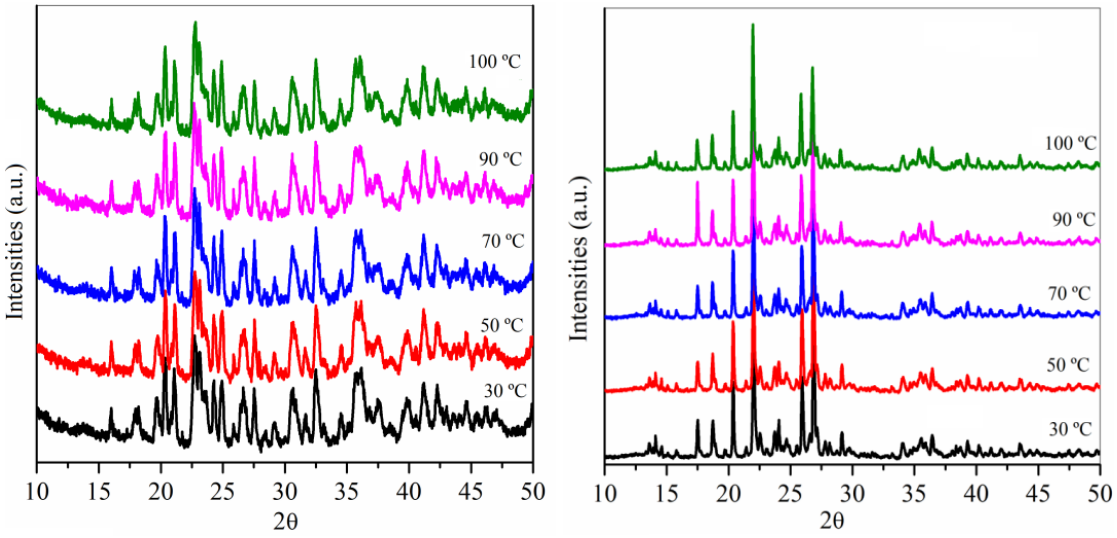

(a) (b)

Figure 5.8 VT-PXRD pattern of Famotidine (a) and FAM.THP cocrystal (b).

FAM.THP is crystallized out from methanol and solve with the triclinic space group $P\bar{1}$. The asymmetric unit consists of one molecule of FAM and two molecules of THP. In the crystal lattice of FAM.THP two molecules of FAM involve in $R_2^2(12)$ sulphonamide type homodimer motif formation via N−H···O hydrogen bond interaction (Figure 5.9). This sulphonamide dimer is further connected to the *endo* carbonyl group of two THP molecules through N−H···O hydrogen bond synthon to form a two-dimensional sheet. The imidazole N–H and *exo*-carbonyl O of THP is involved in the formation of $R_2^2(9)$ intermolecular heterosynthon with famotidine molecule through N–H···N and N–H···O interactions. Two symmetry independent theophylline molecules form $R_2^2(8)$ heterodimer via C–H···O and N–H···N hydrogen bond (Figure 5.9). The unit cell parameters are tabulated and given in Appendix Table A.8. Suitable single crystal could not be isolated for data collection of FAM.CAF and FAM.THB despite several attempts.

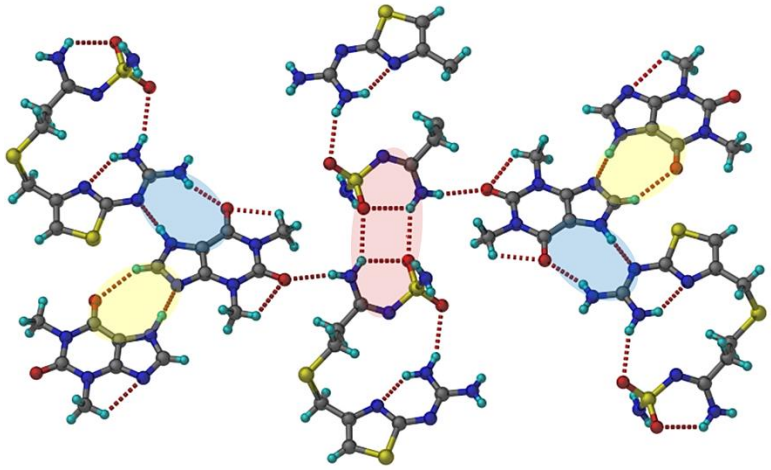

Figure 5.9 $R_2^2(12)$ homodimer (red circle) and $R_2^2(9)$ heterodimer (blue circle) involved in the formation of FAM.THP.

Table 5.3 Hydrogen bond parameters of SCXRD structure of cocrystal THP.FAM

Cocrystal	Interaction	H···A/Å	D···A/Å	∠D–H···A/ Å	Symmetry Code
	N_{10}–H_{4A}···O_7	2.13	2.863 (2)	161	x,y,1+z
	N_{10}–H_{5A}···O_3	2.08	2.908 (2)	172	1-x,-y,1-z
	N_{11}–H_{8A}···O_6	2.29	3.094(2)	156	–
	N_{13}–H_{10A}···O_1	2.22	3.018 (2)	168	-1+x,y,z
FAM.THP	N_{13}–H_{12A}···O_5	2.31	3.033 (2)	141	-1-x,-y,1-z
	N_{15}–H_{15A}···N_8	2.24	3.050 (2)	166	-1+x,y,1+z
	N_3–H_{16A}···N_9	1.96	2.893(2)	178	x,y,-1+z
	N_7–H_{17A}···N_4	1.67	2.809 (2)	177	2-x,1-y,-z
	C_{12}–H_{12}···O_4	2.40	3.219 (2)	146	2-x,1-y,-z

5.3.6 Cocrystals Stability

A slurry experiment is performed to examine the phase stability of famotidine and its cocrystals at pH 1.2. Solid materials that are extracted from the slurry at certain time intervals are characterized by FT-IR and PXRD. The PXRD patterns of solid cocrystal materials of FAM.THP, retrieved from slurry retain the original peak position even after 24 hours. This confirmed the phase stability of this cocrystal material at pH 1.2. However, there are significant phase changes observed in PXRD of famotidine slurry within one hour, which is due to its degraded product. The decomposition of famotidine is further confirmed by NMR analysis. Stacked PXRD plots obtained from the slurry of drug famotidine and cocrystal FAM.THP at different time intervals is shown in Figure 5.10.

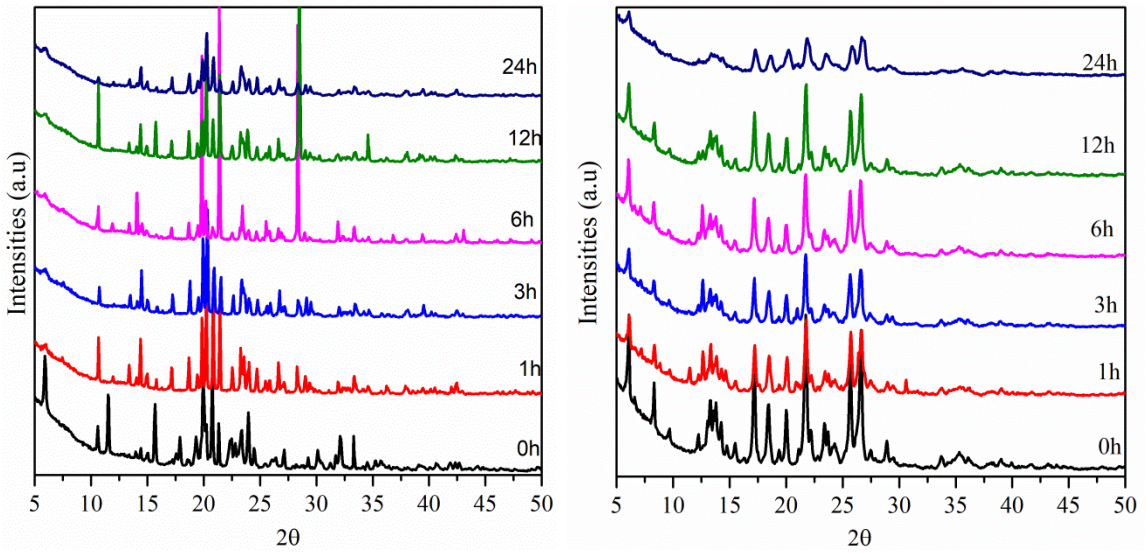

(a) (b)

Figure 5.10 Stacked PXRD patterns of materials obtained from slurry experiments at pH~1.2 up to 24h (a) famotidine and it's (b) cocrystal FAM.THP.

At high acidic condition, the –C=N site of the amidine group of famotidine is susceptible to hydrolysis; which leads towards the formation of the degraded product. The improved stability of FAM.THP cocrystal at pH 1.2 can be attributed to the involvement of the 1º amine of the amidine group of famotidine in the formation of multiple stronger hydrogen bond synthon. This group involves in the $R_2^2(12)$ sulphonamide type homodimer motif via N−H···O hydrogen bond interactions. It is further connected to *endo* carbonyl of THP through strong intermolecular N−H···O hydrogen bond. Formation of these synthons minimizes the susceptibility of acid hydrolysis at the –C=N site of the amidine group by lowering of electrophilic nature of the –C=N carbon. Further, the analysis of the crystal structures of famotidine polymorphs A and B reveals that 1º amine of amidine group does not participate in stronger hydrogen bond interaction. Thus, it makes the –C=N group more exposed to electrophilic attack and famotidine become more prone to acid hydrolysis.

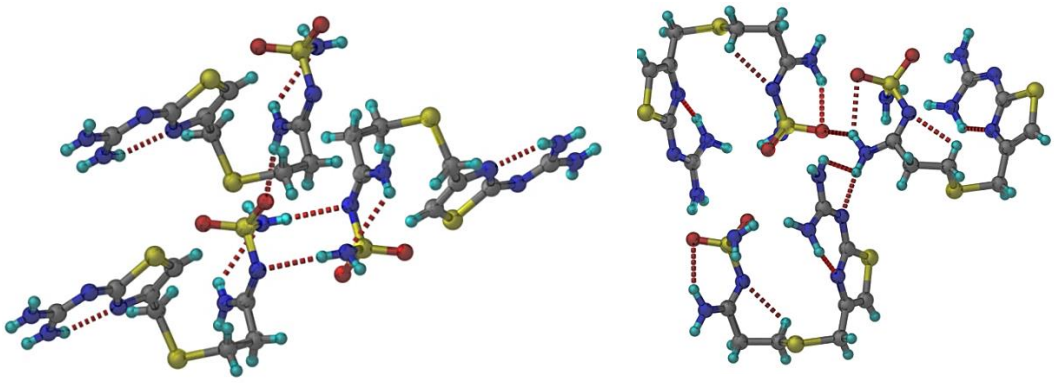

(a) (b)

Figure 5.11 Crystal packing diagram of famotidine polymorphs (a) A and (b) B exposed the –C=N group for acid hydrolysis.

The stability study has also been performed for the cocrystals i.e. FAM.CAF and FAM.THB. A sufficient amount of slurry is retrieved from the solution at different time intervals and PXRD pattern has been recorded.

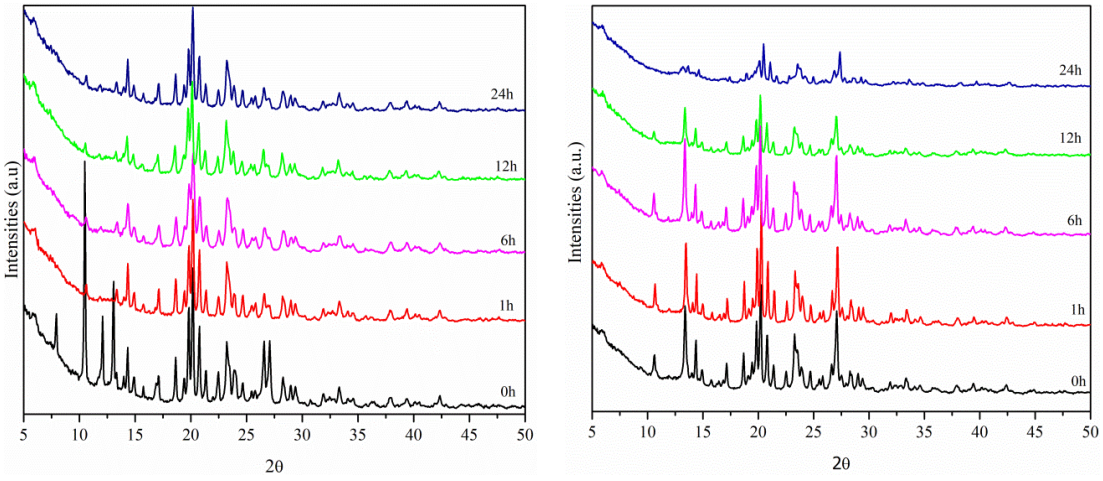

(a) (b)

Figure 5.12 Stacking PXRD patterns of materials obtained from slurry experiments at pH~1.2 up to 24h of cocrystal (a) FAM.CAF and (b) FAM.THB.

The FAM.CAF cocrystal shows insignificant behaviour in slurry experiments. An additional peak appeared at 2θ ~ 9.4 after 8h and became prominent at 24h along with few other changes. The alteration in PXRD pattern with additional peak signified phase change, possibly the formation of a hydrate of caffeine. Cocrystal FAM.THB has not shown any significant change in PXRD pattern up to ~24h. The PXRD patterns of solid

phase material retrieved from slurry experiments at pH~1.2 indicate stability of the material up to 24 hours as we did not observe any appearance or disappearance of a new peak.

5.4 Summary

This chapter demonstrates the use of cocrystal technology as a competent approach to prevent the degradation of drug famotidine in acidic condition. Three different cocrystals are synthesized using xanthine derivatives i.e. theophylline, caffeine and theobromine as coformer. Cocrystals are thoroughly characterized using different analytical techniques. The synthesized cocrystals were subjected to a stability study at pH 1.2. Cocrystal with caffeine is identified to be unstable in the slurry experiment and produces hydrate of caffeine. However, the cocrystals of famotidine with theophylline and theobromine are found to be instrumental in stabilizing famotidine in acidic condition. The cocrystals improved the stability of drug molecule through the formation of different hydrogen bonds with coformer, and consequently inhibit the hydrolysis of the drug. Thus, cocrystallization offers a viable route to stabilized drug degradation.

5.5 Experimental section

5.5.1 Materials

Famotidine (purity~98%), caffeine (purity~98%), theophylline (purity~99%) and theobromine (purity~98%) were purchased from Sigma Aldrich and used as received. HPLC-grade solvents such as methanol, isopropanol, acetonitrile, nitromethane etc. obtained from Merck, India were used for without further purification. Deuterated solvents (DMSO-d_6, 99.9%) used for NMR studies were obtained from Sigma-Aldrich. Double distilled water was used to prepare the solution for accomplishing the pharmacokinetic experiments.

5.5.2 *Preparation of FAM*_D

The decomposed material of famotidine was prepared by slurry experiment. 40 mg of famotidine was taken in a conical flask with the addition of 2-3ml of pH~ 1.2 HCl solutions for 1h. The resulting material was filtered and dried out. The material was characterized using different analytical techniques such as DSC, FT-IR, NMR and XRD.

5.5.3 Preparation of Cocrystals

Famotidine cocrystals FAM.CAF, FAM.THP and FAM.THB were synthesized by using liquid assisted mechanochemical grinding. 1:1 ratio of famotidine and their respective coformer result in FAM.CAF and FAM.THB. The cocrystal FAM.THP was prepared by taking FAM and THP in a stoichiometric ratio of 1:2. To prepare the cocrystals, particular materials were taken in a mortar and grinded for 45-60 minutes with dropwise addition of methanol. The grinded material was then transferred to a conical flask and dissolved in methanol at warm condition and kept for crystallization at room temperature. Crystal suitable for single crystal data collection appeared within 2-3 days. The cocrystals were further characterized using DSC, FT-IR and XRD techniques.

5.5.4 Vibrational Spectroscopy

It is one of the important analytical methods which can provide information about the environment of different functional groups of product materials and helps to identify the unknown structure. Therefore, a small amount of solid materials were mixed with 1% KBr powder and subsequently grounded to reduce the size and recorded FTIR spectra using Perkin Elmer Frontier MIR FT-IR spectrophotometer ranging from 450-4000 cm^{-1}. All major stretching vibrational frequencies of the materials are assigned as follows in cm^{-1}: **FAM:** 3505 (N–H), 3102 (=C–H), 1638 (C=N), 1143 (SO_2), 987 (N–S); **FAM_D:** 3470 (N–H), 1684 (C=O); **FAM.CAF**: 3399 (N–H), 1706 (C=O), 1526 (C=N), 1131 (SO_2), 975 (N–S); FAM.THP**:** 3409 (N–H), 1695 (C=O), 1139 (SO_2), 982 (N–S); **FAM.THB**: 3406 (N–H), 1697 (C=O), 1153 (SO_2), 983 (N–S).

5.5.5 Thermal Analysis

Differential scanning calorimetry (DSC) thermograms of all the materials were recorded using Mettler Toledo DSC 822e module. An amount of 5-6mg solid materials were placed in crimped but vented aluminium sample pans and analyzed their thermal stability within the range of temperature 25-300 ºC at the heating rate of 5 ºC min^{-1}. The details of the thermal analysis are described in the result and discussion section. All the samples were purged with a stream of dry N_2 flowing at 150 $mLmin^{-1}$. The instrument was calibrated before starting the sample measurements using pure indium melting at 156.6 ºC and of 25.45 Jg^{-1} for temperature and heat flow accuracy.

5.5.6 Powder X-ray Diffraction (PXRD)

PXRD analysis of all the samples was obtained on a Bruker D8 Focus X-ray diffractometer, Germany. The measurement condition was taken as follows: anode material Cu-Kα X-radiation, λ = l. 54056 Å at 25mA within the range of 2θ at 5–50°. In VT-PXRD experiments reflections were collected at 10 °C intervals from 30 to 100 °C by heating at 1 °C min^{-1}. Diffraction patterns were collected in the 2θ range of 10–50°.

5.5.7 Single Crystal X-ray Diffraction (SCXRD)

X-ray reflections are collected on a Bruker APEX-II, CCD diffractometer using Mo Kα (λ = 0.71073 Å) radiation. Data reduction is performed using Bruker SAINT Software [23]. Intensities for absorption are corrected using SADABS. Structures are solved and refined using SHELXL-2014 with anisotropic displacement parameters for non-H atoms [24]. Hydrogen atoms on O and N are experimentally located in all crystal structures. All C–H atoms are fixed geometrically using the HFIX command in SHELX-TL. X-Seed is used to prepare figures and packing diagrams [25]. A check of the final CIF file using PLATON did not show any missed symmetry [26,27]. The hydrogen bond distances in the X-ray crystal structures (Table 5.3) are neutron-normalized by fixing the D–H distance to its accurate neutron value (O–H 0.983 Å, N–H 1.009 Å, C–H 1.083 Å).

5.5.8 NMR Spectroscopy

^{1}H & ^{13}C-NMR spectra of all the materials were performed on a JEOL JNM-ECS FTNMR equipped with a 5 mm SB dual ^{1}H/^{13}C probe and Delta software.

FAM: ^{1}H-NMR (400 MHZ, DMSO-d_6): 8.24 (s, 1H), 7.34 (s, 1H), 6.83 (s, 4H), 6.50 (s, 2H), 3.62 (s, 2H), 2.70–2.66 (t, *J*= 8 Hz, 2H) and 2.45–2.41 (t, *J*=7.2, 2H).

^{13}C-NMR (100 MHZ, DMSO-d_6) of FAM: 171.6, 165.3, 156.4, 148.1, 106.1, 36.2, 30.9, 27.9.

FAM_D: (^{1}H-NMR, 400 MHZ, DMSO-d_6): 8.29 (s, 1H), 7.33 (s, 2H), 6.66 (s, 4H), 3.40 (s, 4H), 2.73–2.71 (t, *J*=8 Hz, 2H), 2.50–2.48 (t, *J*=4 Hz, 2H).

^{13}C-NMR (100 MHZ, DMSO-d_6) FAM_D: 175.5, 165.2, 157.1, 147.9, 104.7, 36.3, 31.4, 28.1

5.5.9 Phase Stability

Physical stability of famotidine and its cocrystals were examined at *p*H ~1.2 HCl condition using a slurry experiment. An excess amount of samples were taken in a beaker and 3-4 mL of HCl solution was poured into it and kept stirring at room temperature. A small amount of slurry was retrieved in specific time interval i.e. 1 h, 3 h, 6 h and 24 h recorded their FT-IR and PXRD pattern.

5.6 References

[1] Yanagisawa, I., Hirata, Y., and Ishii, Y. Studies on Histamine H2Receptor Antagonists. 2. Synthesis and Pharmacological Activities of N-Sulfamoyl and N-Sulfonyl Amidine Derivatives. *Journal of Medicinal Chemistry*, 30(10):1787-1793, 1987.

[2] Langtry, H. D., Grant, S. M., and Goa, K. L. Famotidine. An updated review of its pharmacodynamic and pharmacokinetic properties, and therapeutic use in peptic ulcer disease and other allied diseases. *Drugs*, 38(4):551-590, 1989.

[3] Campoli-Richards, D. M. and Clissold, S. P. Famotidine. Pharmacodynamic and pharmacokinetic properties and a preliminary review of its therapeutic use in peptic ulcer disease and Zollinger-Ellison syndrome. *Drugs*, 32(3):197-221, 1986.

[4] Dammann, H.-G., Müller, P., and Simon, B. 24 Hour Intragastric Acidity and Single Night-time Fose of Three H2-blockers. *The Lancet*, 322(8358):1078, 1983.

[5] Amidon, G. L., Lennernäs, H., Shah, V. P., and Crison, J. R. A theoretical basis for a biopharmaceutic drug classification: the correlation of in vitro drug product dissolution and in vivo bioavailability. *Pharmaceutical research*, 12(3):413-420, 1995.

[6] Olea-Azar, C. and Parra-Mouchet, J. Conformational studies on 2-guanidinylthiazole, famotidine and some analogues. *Journal of Molecular Structure: THEOCHEM*, 390(1-3):239-245, 1997.

[7] Singh, S., Kumar, S., Sharda, N., and Chakraborti, A. K. New findings on degradation of famotidine under basic conditions: Identification of a hitherto unknown degradation product and the condition for obtaining the propionamide intermediate in pure form. *Journal of Pharmaceutical Sciences*, 91(1):253-257, 2002.

[8] Slovensko kemijsko društvo., E. S., Zaazaa, H. E., Soudi, A. T., and Salem, M. Y. Development and Validation of Chromatographic Methods for Simultaneous Determination of Ibuprofen and Famotidine in Presence of Related Substances in

Pharmaceutical Formulations. *Acta Chimica Slovenica*, 62(1):45-51, 2014.

[9] Mady, F. M., Abou-Taleb, A. E., Khaled, K. A., Yamasaki, K., Iohara, D., Taguchi, K., Anraku, M., Hirayama, F., Uekama, K., and Otagiri, M. Evaluation of carboxymethyl-β-cyclodextrin with acid function: Improvement of chemical stability, oral bioavailability and bitter taste of famotidine. *International Journal of Pharmaceutics*, 397(1-2):1-8, 2010.

[10] Suleiman, M. S., Najib, N. M., Hassan, M. A., and Abdel-Hamid, M. E. Kinetics of the acid-catalyzed hydrolysis of famotidine. *International Journal of Pharmaceutics*, 54(1):65-69, 1989.

[11] Melo, S. R. d. O., Homem-de-Mello, M., Silveira, D., and Simeoni, L. A. Advice on Degradation Products in Pharmaceuticals: A Toxicological Evaluation. *PDA Journal of Pharmaceutical Science and Technology*, 68(3):221-238, 2014.

[12] Trask, A. V., Motherwell, W. D. S., and Jones, W. Physical stability enhancement of theophylline via cocrystallization. *International Journal of Pharmaceutics*, 320(1-2):114-123, 2006.

[13] Trask, A. V., Samuel Motherwell, W. D., and Jones, W. Pharmaceutical cocrystallization: Engineering a remedy for caffeine hydration. *Crystal Growth and Design*, 5(3):1013-1021, 2005.

[14] Duggirala, N. K., Perry, M. L., Almarsson, Ö., and Zaworotko, M. J. Pharmaceutical cocrystals: along the path to improved medicines. *Chemical Communications*, 52(4):640-655, 2016.

[15] Bolla, G. and Nangia, A. Pharmaceutical cocrystals: walking the talk. *Chemical Communications*, 52(54):8342-8360, 2016.

[16] Babu, N. J., Sanphui, P., and Nangia, A. Crystal engineering of stable temozolomide cocrystals. *Chemistry - An Asian Journal*, 7(10):2274-2285, 2012.

[17] Wang, J. R., Zhou, C., Yu, X., and Mei, X. Stabilizing vitamin D_3 by conformationally selective co-crystallization. *Chemical Communications*,

50(7):855-858, 2014.

[18] Lu, J., Wang, X. J., Yang, X., and Ching, C. B. Polymorphism and crystallization of famotidine. *Crystal Growth and Design*, 7(9):1590-1598, 2007.

[19] Russo, M. G., Brusau, E. V., Ellena, J., and Narda, G. E. Solid-state supramolecular synthesis based on the N-H...O heterosynthon: An approach to solve the polymorphism problem in famotidine. *Journal of Pharmaceutical Sciences*, 103(11):3754-3763, 2014.

[20] Shi, X., Gao, J., Liu, Z., Zhang, J., and Gao, Y. Enhanced dissolution of famotidine by cocrystal formation with tartaric acid and maleic acid. *Journal of China Pharmaceutical University*, 44(2):124-129, 2013.

[21] Islam, M. S. and Narurkar, M. M. Solubility, stability and ionization behaviour of famotidine. *The Journal of pharmacy and pharmacology*, 45(8):682-686, 1993.

[22] *SAINT Plus, Bruker AXS Inc.:* Madison, WI. 2008.

[23] *BRUKER AXS (v 6.14); Bruker AXS Inc.:* Madison, WI. 2008.

[24] L. J. Barbour *X–Seed, Graphical Interface to SHELX–97 and POVRay*, University of Missouri–Columbia. 1999.

[25] Spek, A. L. *PLATON, A Multipurpose Crystallographic Tool*, Utrecht University, Utrecht, Netherland. 2002.

[26] Spek, A. L. and IUCr Single-crystal structure validation with the program *PLATON*. *Journal of Applied Crystallography*, 36(1):7-13, 2003.